SOME PECULIARITIES OF RESONANCE TUBE GAS-DYNAMICAL HEATING

Danton J.F.Villas Boas – danton@iae.cta.br
Khoze Kessaev
Mario Niwa - niwa@iconet.com.br
Instituto de Aeronáutica e Espaço - IAE
Centro Técnico Aeroespacial
12228-904 - São José dos Campos - SP - Brasil

Abstract. *It is known that an underexpanded gas jet entering into a thin-wall cylindrical cavity (resonance tube) can cause fast and strong heating of the walls, up to a temperature which can exceed several times the gas jet stagnation temperature (Sprenger, 1954). Recently, an application of this phenomenon used for ignition of rocket-engine gas and liquid propellants was proposed by Niwa et al., 2000, since the temperature inside the resonance tube can achieve values large enough to ignite the propellant mixture. In the present work, a summary of the resonance tube theoretical model (Kessaev, 1990) is presented and not obvious peculiarities of tube wall heating are revealed. Results from a theoretical model are compared with those from experiments. Characteristics such as tube length effect, temperature distributions along the tube wall and location of maximum temperature region are studied in detail.*

Keywords: resonance tube, propellant ignition, shock waves, gas-dynamical heating.

1. INTRODUCTION

It was Hartmann (1922) who discovered that underexpanded gas jets could produce high intensity wave oscillations by interaction with a cavity. Sprenger (1954) determined that thermal effects accompany oscillations in deep cavities by. The temperature attained in the bottom of the cavity was greater by several times the gas jet total temperature and could achieve 1000 to 1200 K. Since that time a number scientists worked on this phenomenon and investigations leading to different aspects of it were found. Some experimental results for the resonance tube effect were presented by (Thompson, 1964). The fluid dynamics of resonance tubes was presented by (Brocher et al., 1970). From 1970 to 1977 some applications of this effect were proposed for rocket engine ignition (Phillips et al., 1970), (Marchese et al., 1973) and (Przirembel et al., 1977). In 1990 a simplified model of the interaction jet-cavity was described (Kessaev, 1990). Today the resonance tube gas-dynamical heating provokes again considerable interest for rocket propellant ignition (Niwa et. Al., 2000), since the temperature inside the resonance tube can quickly achieve values more than enough to provides oxygen mixtures ignition.

Figure 1 shows one of the possible ignition schemes based on the thermal effect of the deep cavity. Gaseous oxidizer and fuel are injected through nozzle into the resonance tube and are heated and ignited there. The flame leaves the resonator cavity and ignites the liquid propellant in the engine combustion chamber.

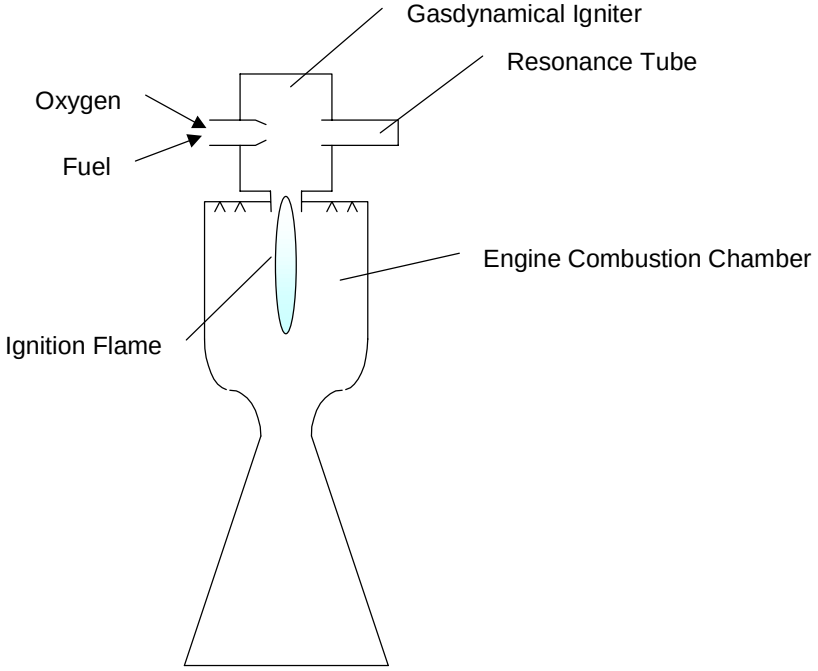

Figure 1 – One of the Possible Schemes of Gas-Dynamic Ignition

The idea in the use potential energy of compressed gas for multiple ignition of rocket engine seems very attractive due to the simplicity of the gas-dynamic igniter scheme. A fundamental understanding of the mechanisms of gas-dynamic heating and its correlation with the geometric parameters of the "gas-cavity" system are very important tasks for the calculation and design of engine igniters.

In the present work an attempt is made to experimentally verify some not obvious peculiarities of the gas-dynamic heating, which were detected by the development of the theoretical aspects described by Kessaev (1990).

2. THEORETICAL ASPECTS OF THE GAS-DYNAMICAL HEATING

Figure 2a shows the moment when the cavity inlet is already filled by the underexpanded entering gas, pressing the internal gas as if it were a piston. CS *(Contact Surface)* marks the surface of both gases interaction. It is assumed that there is no effect of mixing on the CS, therefore the gas velocity and pressure have no discontinuity and are the same on both sides of the CS. This can be possible if ahead of the CS the intensity of the shock wave velocity, W_w, results in an increase of the internal gas pressure P_1 to the external gas static pressure P_2 and increases the gas velocity from the initial value W_1 to the invaded gas velocity value W_{cs} as the CS moves downstream.

After reaching the blind end of the cylinder, the shock wave with velocity W_w is reflected and moves in the opposite direction with velocity W_r (Figure 2b). It interacts with the disturbed internal gas, meets the still entering gas and makes it stagnant. This is why there exists the

cavity section ΔL located in the blind end region of the cylinder. It is filled with internal gas compressed by the pressure P_3, and the entering gas does not penetrate into it at all (Figure 2c). Moreover, if P_3 is greater than the jet stagnation pressure P_0, the internal gas will push the external gas out, discharging the cavity with an ejection effect. When the ejection phase ends, the pressure in the tube will fall to some value $P_1^{(2)}$ and the jet parameters P_2 and W_2 at the tube inlet will be restored.The entering process will begin again with $P_1 = P_1^{(2)}$, and so forth in the form of self-sustained oscillations. The index $^{(2)}$ corresponds to the end of the first "compression-expansion" cycle, in other words $T_1^{(2)}$ and $P_1^{(2)}$ are the initial gas parameters for the second cycle.

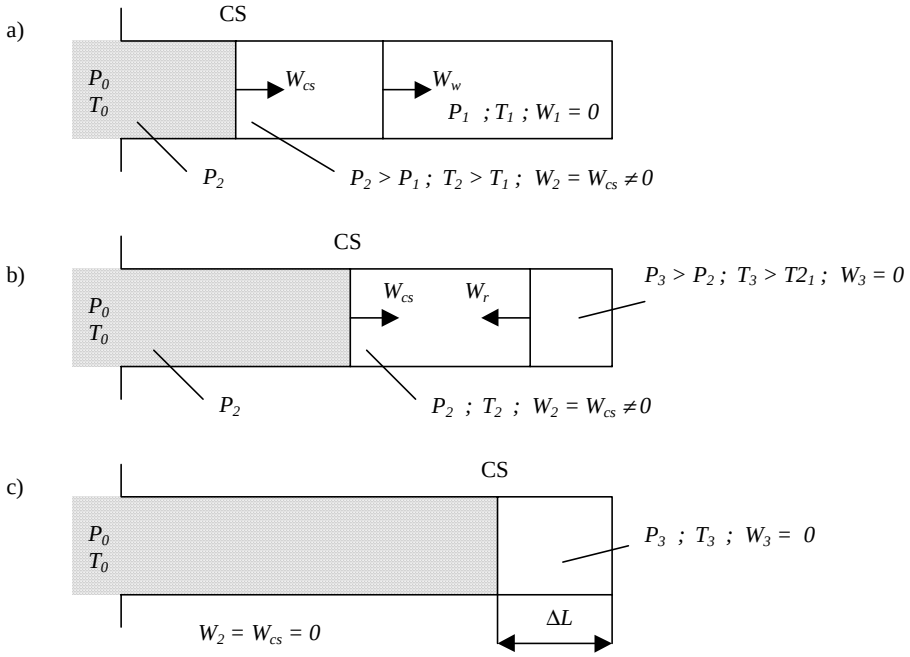

Figure 2 – Process of Invaded and Enclosed Gases Interaction

That kind of interaction of the jet with the cylinder tube is expressed by following equations (Kessaev, 1990):

Entering gas inlet velocity:

$$W_2 = \sqrt{\frac{2k}{k-1} R.T_0 \left[1 - \left(\frac{P_2}{P_0}\right)^{\frac{k-1}{k}}\right]} \equiv W_{cs} \qquad (1)$$

Pressure ratio as a result of shock wave passage:

$$\frac{P_2}{P_1} = \frac{2k.\left(\frac{W_w}{a_1}\right)^2 - (k-1)}{k+1} \qquad (2)$$

Internal gas sound velocity in:

$$a_1 = \sqrt{kRT_1} \tag{3}$$

Shock wave velocity:

$$W_w = \frac{a_1}{2}\left[\frac{k+1}{2}\frac{W_2}{a_1} + \sqrt{\left[\frac{(k+1)W_2)}{2a_1}\right]^2 + 4}\right] \tag{4}$$

Pressure ratio as a result of the reflected wave passage:

$$\frac{P_3}{P_1} = \frac{(3k-1)\frac{P_2}{P_1} - (k-1)}{(k+1)\frac{P_1}{P_2} + (k-1)} \tag{5}$$

With consideration that the shock wave can be born only when:

$$\frac{P_0}{P_1} \geq \left(\frac{k+1}{2}\right)^{\frac{k}{k-1}} \tag{6}$$

and also that the external gas velocity inside the tube can not exceed the critical value:

$$W_2 \leq \sqrt{\frac{2k}{k+1}RT_0} = W_{cr} \tag{7}$$

Equations (1) to (5) permit to calculate under what conditions the shock wave oscillations will take place (i.e. $P_3 > P_0$). So, with $T_0 = T_1 = 293$ K and $k = 1.4$ the oscillations occur for $P_0 / P_1 \geq 1.89$ and die away for $P_0 / P_1 \geq 5.9$. The relatively small range of permissible values allows to call the cavity as “resonator” or “resonance tube”. Figure 3 shows the rage of permissible solutions in the interval $1.89 \leq P_0 / P_1 \leq 5.9$.

Both the generated and reflected shock waves heat the gas enclosed in the tube:

$$\frac{T_2}{T_1} = \left[\frac{(k+1)+(k-1)\frac{P_2}{P_1}}{(k+1)+(k-1)\frac{P_1}{P_2}}\right] \tag{8}$$

$$\frac{T_3}{T_1} = \frac{T_2}{T_1} \cdot \left[\frac{(k+1) + (k-1)\frac{P_3}{P_2}}{(k+1) + (k-1)\frac{P_2}{P_3}} \right] \qquad (9)$$

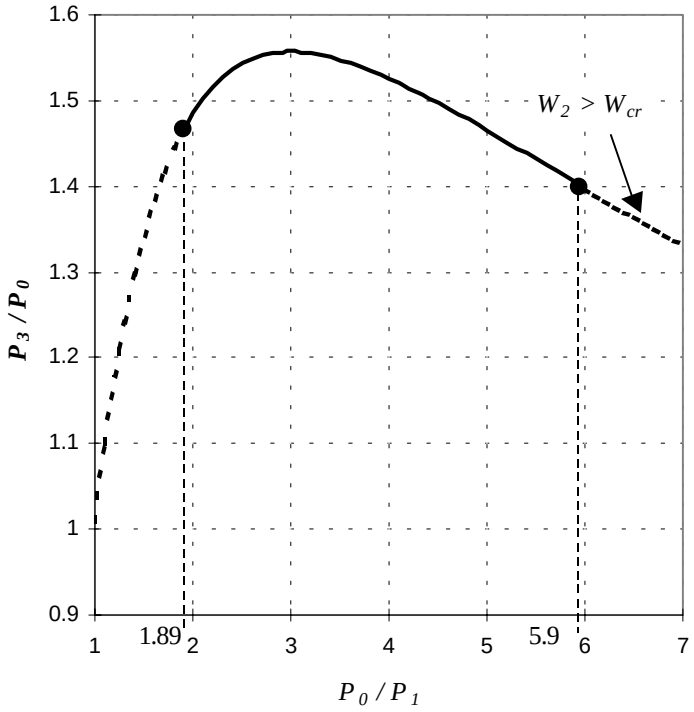

Figure 3 – Diagram of Shock Wave Oscillations Occurrence
for $T_1 = T_0 = 293$ K and $k = 1.4$

By isoentropical expansion to $P_1^{(2)}$ the gas is cooled to some temperature $T_1^{(2)}$:

$$T_1^{(2)} = T_3 \left(\frac{P_1^{(2)}}{P_3} \right)^{\frac{k-1}{k}} \qquad (10)$$

The realization of “compression-expansion” cycles in consecutive order leads to gradual heat accumulation.

Analysis of Equations (1) to (10) shows that the maximal rate of heating takes place when:

$$\frac{P_2}{P_0} = \left(\frac{2}{k+1} \right)^{\frac{k}{k-1}} \qquad (11)$$

To achieve this the cavity inlet should be located in such place of the jet where the gas velocity is critical, i.e. $W_2 = W_{cr}$.

3. PECULIARITIES OF THE GAS-DYNAMICAL HEATING

Further investigation of the above described model allows to emerge some features of the jet-cavity interaction. The diagram on Figure 4 illustrates an idealized scheme of the movement of the contact surface CS, generated shock wave with velocity W_w, and reflected shock wave with velocity W_r, inside a cylinder of length L_r. Starting the process, the jet enters the cylinder and travels the distance 0-L_0.At the point L_0, it is assumed that the shock wave is completely formed. The entering gas continues its propagation until it is stopped by the reflected shock wave in L_s cross-section in a time interval t_s.

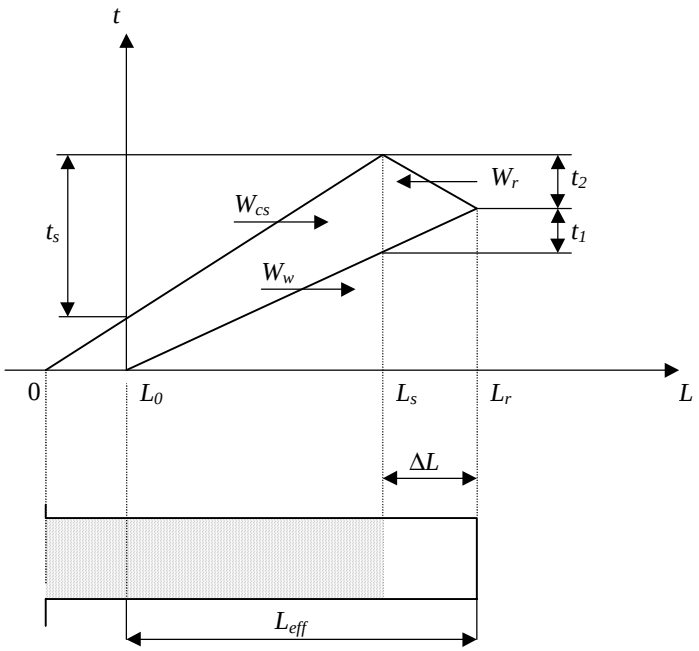

Figure 4 – Idealized Scheme of the Contact Surface and Shock Waves Movement Inside Tube

In this event:

$$t_s = \frac{L_r - L_0 - \Delta L}{W_{cs}} = \frac{L_{eff} - \Delta L}{W_{cs}} \tag{12}$$

Where L_{eff} : effective length of the tube.

The time interval t_s is required for the shock wave reach the blind end of the tube and return back to L_s as a reflected wave:

$$t_s = \frac{L_{eff}}{W_w} + \frac{\Delta L}{W_r} \tag{13}$$

where W_r is the reflected wave velocity relative to the tube walls:

$$W_r = W_{rg} - W_{cs} \tag{14}$$

where W_{rg} is the reflected shock wave velocity relative to the gas flow coming through it; from shock wave theory:

$$W_{rg} = a_2 \sqrt{\frac{(k+1)\frac{P_3}{P_2} + (k-1)}{2k}} \tag{15}$$

$$a_2 = \sqrt{kRT_2} = \sqrt{kRT_1 \left[\frac{(k+1) + (k-1)\frac{P_2}{P_1}}{(k+1) + (k-1)\frac{P_1}{P_2}} \right]} \tag{16}$$

$$\frac{P_3}{P_2} = \frac{(3k-1) - (k-1)\frac{P_1}{P_2}}{(k-1) + (k+1)\frac{P_1}{P_2}} \tag{17}$$

From Equations (12) and (13) it follows:

$$\Delta L = L_{eff} \frac{1 - \frac{W_{cs}}{W_w}}{1 + \frac{W_{cs}}{W_r}} \tag{18}$$

Figure 5 illustrates the dependence ΔL / L_{eff} on T_3 obtained from the system of Equations (1) to (18) solved for air at T_0 = 293 K, k = 1.4, and P_2 / P_0 = 0.529 and shows the first gas-dynamic heating peculiarities:

a) the length of the cavity section ΔL occupied by the heated gas comprises 20-25% of L_{eff} at the initial stage of heating (T_3 = 550 to 600 K).
b) the section ΔL grows up and reaches 35% of L_{eff} with heating up to T_3 = 900 K.

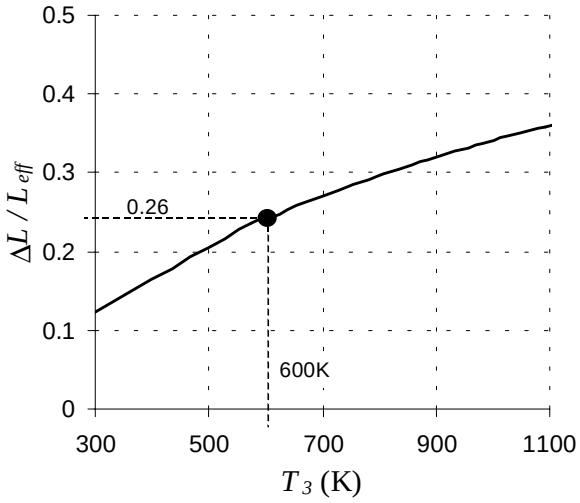

Figure 5 – Dependence of ΔL / L_{eff} Ratio from Temperature T_3

In a real process the heat transfer takes place: gas heats the tube walls. At the cross - section L_s the gas interacts with the wall surface during $t_1 + t_2$ time period required for the shock and reflected waves to cover the distance from L_s to L_r towards and back. The amount of heat Q_s absorbed by the surface in L_s is directly proportional to the temperature T_2 and duration of contact $t_1 + t_2$:

$$Q_s \sim T_2\left(t_1 + t_2\right)$$

In section L_r the amount of heat Q_r absorbed by the surface during a time interval equal to t_2 is directly proportional to the product of T_3 by t_2:

$$Q_r = T_3 t_2$$

Since $t_1 = \Delta L / W_w$ and $t_2 = \Delta L / W_r$:

$$\frac{Q_s}{Q_r} = \frac{T_2}{T_3}\left(1 + \frac{W_r}{W_w}\right) \tag{19}$$

Figure 6 shows the dependence of Q_s / Q_r on T_3 obtained from the system of Equations (1) to (19) solved for air. We can see that $Q_s / Q_r > 1.0$. In other words, in the tube cross section L_s (where $W_{cs} = 0$) heat absorption is a maximum. So, Figure 6 demonstrates one more peculiarity of heating:

c) the walls of the resonance tube in the section ΔL are heated non-uniformly presenting a maximum temperature at the cross-section L_s.

From the joint analysis of Figure 5 and Figure 6 also follows:

d) the length of ΔL is decreased with short length resonance tubes and shock waves heating becomes impossible when ΔL tends to 0;

e) during the gas heating the section ΔL expands, and the location of the maximum temperature displaces to the cavity inlet side.

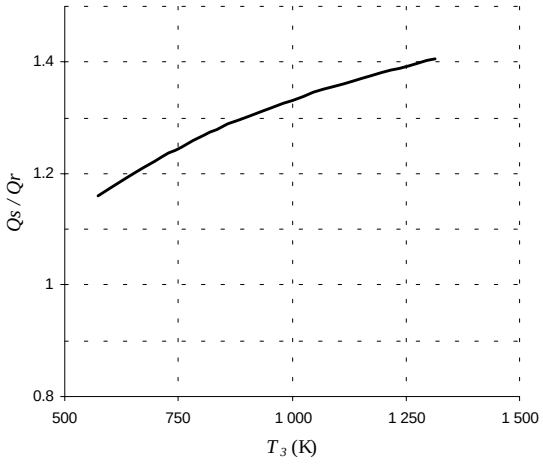

Figure 6 – Dependence of Q_s / Q_r ratio from T_3 Temperature

4. EXPERIMENTAL CHECKING OF THEORETICAL DEDUCTIONS

The above theoretical computations were confirmed by a simple experiment, which is shown schematically in Figure 7. The test sample is composed by a stainless steel blind-end tube, with internal diameter (d_r) of 8.0 mm and the segmented design allows to vary its length.

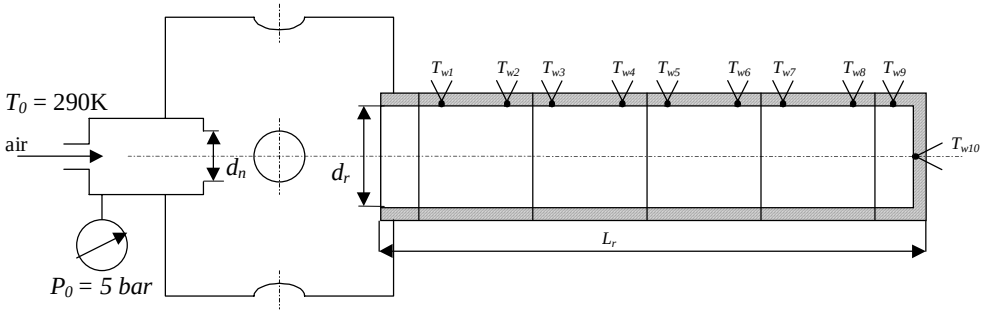

Figure 7 – Scheme of Test Apparatus

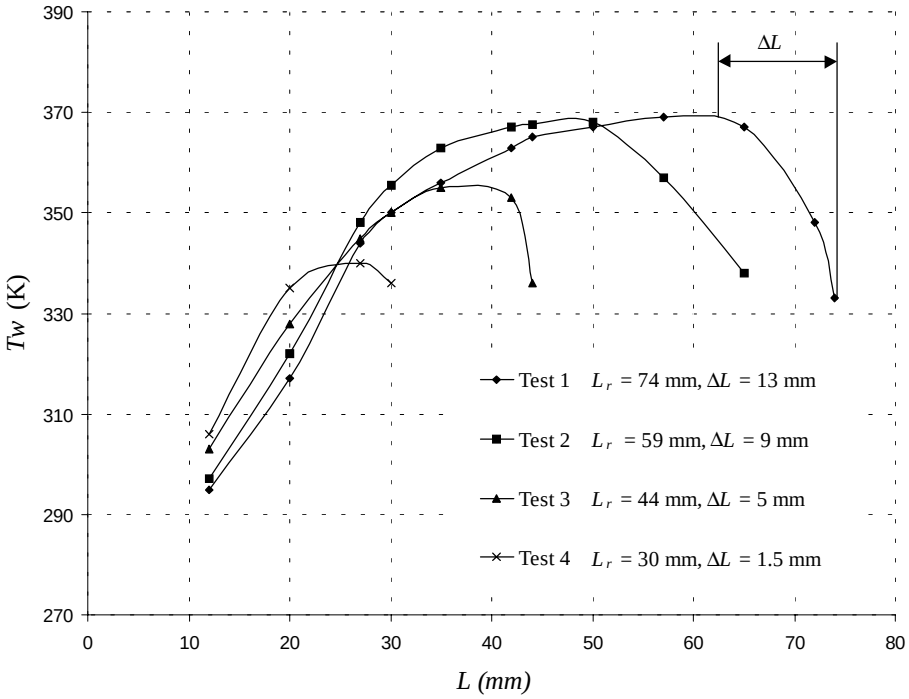

Figure 8 – Wall Temperature Measurements from Tests

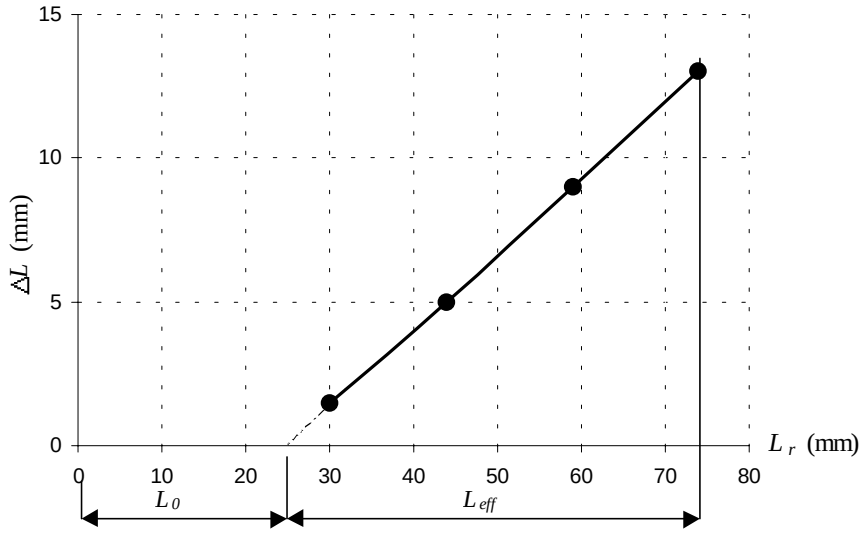

Figure 9 – Dependence of ΔL on L_r

The distance between the tube inlet and the nozzle was 8.0 mm. The diameter of the nozzle (d_n) was 5.0 mm. The cavity depths were 74 mm, 59 mm, 44 mm and 30 mm. Thermocouples were fixed at a distance of 1.0 mm from the tube inner surface in order to measure the wall temperature distribution along the tube. Air was supplied with a temperature of 290 K and pressure of 5 bar.

Figure 8 presents the experimental wall temperature (T_w) distributions in the initial stage of heating corresponding to different values of tube length. One can see that:

- the walls near the blind end of the tube are heated in a non-uniform manner and the location of the temperature maximum is displaced from the blind end (peculiarity "c").
- the distance between the blind end and the temperature maximum location is shortened as the tube depth L_r decrease (peculiarity "d").

Figure 9 shows the experimental dependence of ΔL from the resonance tube depth L_r . Extrapolation to a point where $\Delta L = 0$ reveals the tube cross section L_0 where shock wave is formed. In such case $L_{eff} = L_r - L_0$ and $\Delta L / Leff = 0.26$ (peculiarity "a").

5. CONCLUSION

Experimental observations reinforce the fundamental tenets of the theoretical model described in (Kessaev, 1990). The peculiarities founded after calculation of the theoretical model were confirmed by the experimental values. The main conclusions are that the walls near the blind end of the tube are heated in a non-uniform manner and the location of the temperature maximum is displaced from the blind end, and is located at a distance of ΔL. The distance between the blind end and the temperature maximum location is shortened as the tube depth L_r decreases, up to a limiting distance where the gas dynamic oscillations vanish.

ACKNOWLEDGEMENTS

The second and the third authors would like to acknowledge FAPESP for the financial support during the conduction of the present work.

REFERENCES

Brocher, E., Maresca, C., Bournay, M.H., "Fluid Dynamics of the Resonance Tube, Journal of Flid Mechanics, Vol 43, 1970, pp. 369-384

Hartmann, J., "On a New Method for the Generation of Sound Waves", Physical Review, Vol.20, 1922, p.p.719-727

Kessaev, K.V., "Theoretical Model of Resonance Tube", Aviationnaja Technica, 1990, p.p. 49-52 (in Russian)

Marchese, V.P., Rakowsky, E.L., Bement, L.J., "A Fluidic Souding Rocket Motor Ignition System", J.Spacecraft, Vol. 10, No. 11, November 1973, pp. 731-734

Niwa, M., Santana Jr., A., Valle, M., Kessaev, K., "Development of a Resonance Igniter for GO2/Kerosene Ignition", AIAA 36th Joint Propulsion Conference, Huntsville, AL, 16-19 July 2000

Phillips, B., Pavli, A.J., Conrad, E.W., "A Resonance Igniter for Hydrogen-Oxygen Combustors", J.Spacecraft, Vol. 5, No. 5, 1970, pp. 620-622

Przirembel, C.E.G., Fletcher, L.S., "Aerothermodynamics of a Simple Resonance Tube", AIAA Journal, Vol. 15, No. 1, January 1977, pp. 101-104

Sprenger, H.S.,"Über Termische Effecte bei Rezonanzröhren", Mitteilungs aus dem Institut für Aerodynamik, E.T.H., Zurich, 1954, p.p. 18-35

Thompson, P.A., "Jet Driven Resonance Tubes", AIAA Journal, Vol. 2 No. 7, July 1964, pp. 1230-1233